Spectral State Space Models

Anonymous Authors[1]

Abstract

This paper studies sequence modeling for prediction tasks with long range dependencies. We propose a new formulation for state space models (SSMs) based on learning linear dynamical systems with the spectral filtering algorithm (Hazan et al., 2017). This gives rise to a novel sequence prediction architecture we call a spectral state space model. Spectral state space models have provable robustness properties for tasks that require long memory, and are constructed with fixed convolutional filters that do not need to be learned. We evaluate these models on synthetic dynamical systems and long-range prediction tasks of various modalities. These evaluations support the theoretical benefits of spectral filtering for tasks that need very long range memory.

1. Introduction

In recent years, transformer models (Vaswani et al., 2017) have become the staple of sequence modelling (Brown et al., 2020; Dosovitskiy et al., 2020; Jumper et al., 2021). Transformer models are naturally parallelizable and hence scale significantly better than Recurrent Neural Networks (RNNs) (Hopfield, 1982; Rumelhart et al., 1985; Elman, 1990). However, attention layers have memory/computation requirements that scale quadratically with context length. Many approximations have been proposed (see (Tay et al., 2022) for a recent survey).

RNNs (Hopfield, 1982; Rumelhart et al., 1985; Elman, 1990) have seen a recent resurgence in the form of state space models (SSM) which have shown promise in modelling long sequences across varied modalities (Gu et al., 2021a; Dao et al., 2022; Gupta et al., 2022; Orvieto et al., 2023; Poli et al., 2023; Gu & Dao, 2023). SSMs use linear dynamical systems (LDS) to model the sequence-to sequence transform by evolving the internal state of the dynamical system. Despite its simplicity, linear systems can capture a rich set of natural dynamical systems in engineering and the physical sciences due to the potentially large number of hidden dimensions. They are also attractive as a sequence model because their structure is amenable to both fast inference and fast training via parallel scans (Blelloch, 1989; Smith et al., 2023) or convolutions (Gu et al., 2021a). These techniques make SSMs suitable for sequence tasks which inherently depend on long contexts that scale poorly for transformers.

However, on tasks that require very long range memory, SSMs can be unstable to train. This issue is specifically highlighted in the work of (Orvieto et al., 2023), who observe that on long range tasks, learning an LDS directly does not succeed and requires interventions such as stable exponential parameterizations and specific normalization, which have been repeatedly used either implicitly or explicitly in the SSM literature (Gu et al., 2021a).

In this work, we consider the problem of sequential prediction tasks that require long range memory from the perspective of learning marginally-stable dynamical systems. Marginally-stable systems have dynamics that do not exhibit decay: their dynamics matrices can have eigenvalues up to 1, allowing the system to memorize information from the far past. The spectral filtering technique proposed by Hazan et al. (2017) can provably learn certain marginally-stable dynamical systems efficiently. It achieves this by projecting the sequence of inputs onto a small subspace constructed using the special structure that arise from learning a discrete LDS. The efficient learning guarantee of spectral filtering indicates that if we featurize the input using the spectral basis, we can potentially design models that are capable of efficiently and stably representing systems with extremely long memory.

1.1. Our Contributions

We start by proposing state space models with learned components that apply spectral filtering for their featurization. Our main contribution is a neural architecture that is based on these spectral state space models. We implement this neural architecture and apply it towards synthetically generated data as well as the Long Range Arena benchmark (Tay et al., 2021). We demonstrate that spectral state space models can

[1]Anonymous Institution, Anonymous City, Anonymous Region, Anonymous Country. Correspondence to: Anonymous Author <anon.email@domain.com>.

Under review by the Workshop on Long-Context Foundation Models (LCFM) at ICML 2024. Do not distribute.

stably and more efficiently learn on sequence modelling tasks with long range dependencies without the need for exponential parameterizations, particular initializations and normalizations.

Preliminaries. We defer most prelminaries to Appendix B, and give the basics here. In sequence prediction, every time $t \in [L]$ the learner is presented an input $u_t \in \mathbb{R}^{d_{\text{in}}}$. The learner A then produces a candidate output $\hat{y}_t$, and the learner then suffers an instantaneous loss of $\|y_t - \hat{y}_t\|^2$ given the real output y_t. The task of the learner is to minimize regret over a benchmark set of learning algorithms $\mathcal{A}$, defined as follows

$$\text{Regret} = \sum_{t=1}^{L} \|y_t - \hat{y}_t\|^2 - \min_{A' \in \mathcal{A}} \sum_{t=1}^{L} \|y_t - \hat{y}_t(A')\|^2,$$

where $\hat{y}_t(A')$ is the output of the algorithm A' at time t. A linear dynamical system has four matrix parameters, $A \in \mathbb{R}^{N \times N}, B \in \mathbb{R}^{N \times d_{\text{in}}}, C \in \mathbb{R}^{d_{\text{out}} \times N}, D \in \mathbb{R}^{d_{\text{out}} \times d_{\text{in}}}$. The system evolves and generates outputs according to the following equations

$$x_t \triangleq A x_{t-1} + B u_t, \qquad \hat{y}_t \triangleq C x_t + D u_t. \tag{1}$$

Thus, an example class of benchmark algorithms $\mathcal{A}$ are all predictors that generate $\hat{y}_t$ according to these rules, for a fixed set of matrices A, B, C, D.

Spectral filtering. Another important set of predictors is one which is inspired by spectral filtering (Hazan et al., 2017). The spectral filtering theory builds an efficient representation for all vectors in the range of the function $\mu : [0,1] \to \mathbb{R}^L$ defined as $\mu(\alpha) \triangleq (\alpha - 1)[1, \alpha, \alpha^2 \ldots]$. To build this representation, define the following Hankel matrix $Z \in \mathbb{R}^{L \times L}$ whose entries are given by

$$Z[i,j] \triangleq \frac{2}{(i+j)^3 - (i+j)} \tag{2}$$

Since Z is a real PSD Hankel matrix, it has an exponentially decaying spectrum. As a result, one can show that for all $\alpha \in [0,1]$ [1], the vector $\mu(\alpha)$ is approximately contained in the subspace spanned by the top eigenvectors of Z.

Let $\{(\sigma_j \in \mathbb{R}, \phi_j \in \mathbb{R}^T)\}_{j=1}^{L}$ be the eigenvalue-eigenvector pairs of Z ordered to satisfy $\sigma_1 \geq \sigma_2 \geq \ldots \geq \sigma_d$. We consider a fixed number K of the above eigenvectors. Algorithms in the spectral filtering class generate $\hat{y}_t$ as follows. For each $k \in K$, we first *project* the input sequence until time t on ϕ_k, leading to a sequence $U_{t,k} \in \mathbb{R}^{d_{\text{in}}}$ defined as $U_{t,k} = \sum_{i=1}^{t} u_{t-i} \cdot \phi_k(i)$. The spectral filtering class is further parameterized by matrices $M_1^u \in \mathbb{R}^{d_{\text{out}} \times d_{\text{in}}}$, $M_2^u \in \mathbb{R}^{d_{\text{out}} \times d_{\text{in}}}$ and a set of matrices $M_1^{\phi}, ..., M_K^{\phi} \in \mathbb{R}^{d_{\text{out}} \times d_{\text{in}}}$. The output at time t is then

$$\hat{y}_t = \hat{y}_{t-1} + M_1^u u_t + M_2^u u_{t-1} + \sum_{k=1}^{K} M_k^{\phi} U_{t,k}. \tag{3}$$

Due to space constraints, we refer the reader to Appendix B for more details on the spectral filtering algorithm.

2. Spectral Transform Unit (STU)

In this section, we use spectral filtering to create a sequence to sequence neural network layer, i.e. given an input sequence $\{u_1 \ldots u_L\} \in \mathbb{R}^{d_{\text{in}}}$, it produces an output sequence $\{y_1 \ldots y_L\} \in \mathbb{R}^{d_{\text{out}}}$. A single layer of STU (depicted in Figure 2) is parameterized by a number K, denoting the number of eigenfactors and matrices $M_1^{\phi+} \ldots M_K^{\phi+}, M_1^{\phi-} \ldots M_K^{\phi-} \in \mathbb{R}^{d_{\text{out}} \times d_{\text{in}}}$, and $M_1^u, M_2^u, M_3^u \in \mathbb{R}^{d_{\text{out}} \times d_{\text{in}}}$. The matrices form the *params* of the layer. Further recall the Hankel matrix $Z \in \mathbb{R}^{L \times L}$ in (2) and let $\{(\sigma_j \in \mathbb{R}, \phi_j \in \mathbb{R}^L)\}_{j=1}^{L}$ be the eigenvalue-eigenvector pairs of Z in descending order. Given an input sequence $\{u_1 \ldots u_L\} \in \mathbb{R}^{d_{\text{in}}}$, we first *project* the input sequence till time t on *fixed* filters ϕ_k, leading to two feature vectors $U_{t,k}^+, U_{t,k}^- \in \mathbb{R}^{d_{\text{in}}}$ defined as

$$U_{t,k}^+ = \sum_{i=0}^{t-1} u_{t-i} \cdot \phi_k(i) \qquad U_{t,k}^- = \sum_{i=0}^{t-1} u_{t-i} \cdot (-1)^i \cdot \phi_k(i).$$

Note that for every k, the sequence of features $U_{1:L,k}$ can be computed efficiently via convolution. The output sequence $\{y_1 \cdots y_L\}$ is then given by

$$\hat{y}_t = \underbrace{\hat{y}_{t-2} + \sum_{i=1}^{3} M_i^u u_{t+1-i}}_{\text{Auto-regressive Component}} \tag{4}$$

$$+ \underbrace{\sum_{k=1}^{K} M_k^{\phi+} \sigma_k^{1/4} U_{t-2,k}^+ + \sum_{k=1}^{K} M_k^{\phi-} \sigma_k^{1/4} U_{t-2,k}^-}_{\text{Spectral Component}}. \tag{5}$$

For completeness we prove the following representation theorem Appendix E, which shows that the above class approximately contains any marginally-stable LDS with symmetric A.[2]

Theorem 2.1. *Given any A, B, C, D such that A is a symmetric matrix with $\|A\| \leq 1$ and given any numbers $K \in \mathbb{I}^+, a \in \mathbb{R}^+$, there exists matrices $M_1^u, M_2^u, M_3^u, M_1^{\phi+} \ldots M_K^{\phi+}, M_1^{\phi-} \ldots M_K^{\phi-} \in$*

[1] in particular all α close to 1, representing marginally stable systems.

[2] We discovered some small but easily fixable errors in the original proof of (Hazan et al., 2017) which we have corrected in our proof

$\mathbb{R}^{d_{\text{out}} \times d_{\text{in}}}$, *such that for all* L *and all sequences* $u_{1:L}$ *satisfying* $\|u_t\| \leq a$ *for all* $t \in [L]$ *the following holds. Let* $y^{\text{LDS}}_{1:L}$ *be the sequence generated by execution of the LDS given by* A, B, C, D *(via (10)) and* $y^{\text{SF}}_{1:L}$ *be the sequence generated by Spectral Filtering (via (5)) using the matrices* $M^u_1, M^u_2, M^u_3, M^{\phi+}_1 \ldots M^{\phi+}_K, M^{\phi-}_1 \ldots M^{\phi-}_K$. *Then for all* $t \in [T]$, *we have that*

$$\|y^{\text{LDS}}_t - y^{\text{SF}}_t\|^2 \leq c \cdot \|B\|_{col} \cdot \|C\|_{col} \cdot L^3 \cdot a \cdot e^{-\left(\frac{\pi^2}{4} \cdot \frac{K}{\log(L)}\right)}$$

where $c \leq 2 \times 10^6$ *is a universal constant and* $\|B\|_{col}$, $\|C\|_{col}$ *are the maximum column norm of the matrices B and C respectively.*

The above theorem in particular ensures for any sequence length L that setting $K = O\left(\log(L) \log\left(\frac{\|B\|_{\text{col}} \cdot \|C\|_{\text{col}} \cdot L \cdot a}{\epsilon}\right)\right)$ there exists a spectral filtering model with K filters that can approximate any LDS up to an error of ϵ. Note that the requirement on the number of filters grows logarithmically in L, highlighting the efficiency of the representation. Due to space limitations, we discuss the runtime scaling of our method and compare it with different methods in the appendix (Section A).

We conduct synthetic experiments on the STU layer in Appendix C, and investigate its behavior for learning an LDS compared to the LRU layer proposed in Orvieto et al. (2023). Our results show that the STU layer is significantly more efficient at learning the LDS, demonstrating the advantages of STU as supported by the theoretical guarantees.

3. Stacked STU

To increase the representation capacity and to maintain the efficiency of prediction through linear dynamical systems, SSMs stack these sequence to sequence transforms into multiple layers. Non-linearities in the model can then be introduced by sandwiching them as layers lying in between these sequence to sequence transforms.

In this paper we closely follow the stacking approach followed by (Orvieto et al., 2023), replacing the LRU layers appropriately by STU layers. A schematic for the resultant multi-layer model is displayed in Figure 1a. In a nutshell, the input sequence is first embedded via a time-invariant embedding function followed by multiple repetitions of alternating STU layers and non-linearities (in particular we use GLU). Finally the resulting output is time-pooled followed by a final readout layer according to the task at hand. This composite model can now be trained in a standard fashion via back-propagation and other commonly used deep-learning optimization techniques.

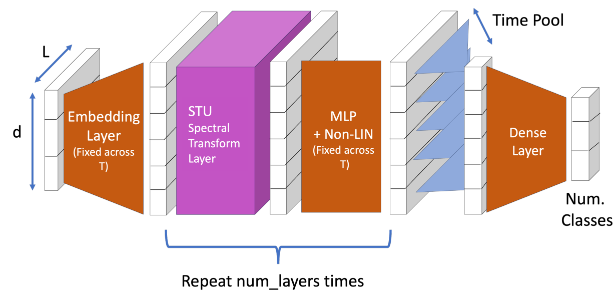

(a) Schematic displaying a multi-layer STU model.

Model	Specification	Pathfinder	PathX
STU	Eqn (5) (K=16)	91.8	89.5
LRU	Dense A	✗	✗
	Λ Exp. Param.	65.4	✗
	Λ Stable Exp.	93.5	✗
	+ Ring Init.	94.4	✗
	+ γ-Norm.	95.1	94.2

(b) Comparison of the basic stacked STU model against LRU ablations in (Orvieto et al., 2023)

3.1. Experiments on Long Range Arena (Tay et al., 2021)

We evaluate the stacked STU model on the Long Range Arena (LRA) benchmark (Tay et al., 2021). This benchmark aims to assess the performance of sequence prediction models in long-context scenarios and consists of six tasks of various modalities, including text and images. SSMs (Gu et al., 2021a) have shown significantly superior performance on most of the tasks compared to Transformer architectures. In particular for the hardest task in the suite, PathX (image classification with context length of 16K), no transformer model has been able to achieve accuracy beyond random guessing. We provide the evaluation of the stacked STU model on the two hardest tasks namely PathFinder and PathX in Table 1b.

We compare our performance against the ablation carried out by (Orvieto et al., 2023) who find that ring initialization, stable exponential parameterization and γ-normalization are all crucial towards learning these tasks. In particular, all three of the above interventions were necessary to learn on PathX to any non-trivial accuracy due to its extremely long context length. On the other hand, we find that the the stacked STU (with the STU component exactly as represented by (5)) is sufficient to learn on both of these tasks to relatively high accuracies. Notably, we do not require any other normalization or initialization techniques. We initialize all the parameters of the STU i.e. M matrices to 0. Details about our implementation as well as details about the experiments including hyperparameters can be found in

	CIFAR	ListOps	Text	Retrieval	Pathfinder	PathX
S4 (Gu et al., 2021a)	88.65	59.60	86.82	90.90	94.20	96.35
LRU (Orvieto et al., 2023)	89	60.2	89.4	89.9	95.1	94.2
AR-STU	**91.34**	**61.14**	**90.47**	90.52	**95.45**	93.24

Table 1: Comparison of the STU model against various proposed SSM models on the LRA benchmark. We report the median over 5 trials for our experiments.

Appendix G. This result in particular highlights the theoretical stability afforded by the STU even under learning tasks involving large sequence lengths. In the appendix (Table 2 we provide the performance evaluation of the stacked STU on all tasks of the LRA benchmark.

4. Hybrid Temporal and Spectral Units

A simple extension to the STU model (Equation (5)) is to parameterize the dependence of y_t on y_{t-2} with a parameter M_y, leading to the following prediction model

$$\hat{y}_t = \underbrace{\boldsymbol{M^y} \hat{y}_{t-2} + \sum_{i=1}^{3} M_i^u u_{t+1-i}}_{\text{Auto-regressive Component}} \tag{6}$$

$$+ \underbrace{\sum_{k=1}^{K} M_k^{\phi+} \sigma_k^{1/4} U_{t-2,k}^{+} + \sum_{k=1}^{K} M_k^{\phi-} \sigma_k^{1/4} U_{t-2,k}^{-}}_{\text{Spectral Component}} . \tag{7}$$

Setting $M^y = I$ we recover the guarantees afforded by Theorem 2.1 and thus the above model is strictly more powerful. We find that the above change leads to significant improvements over the accuracy achieved by the simple STU model, and we can further extend the auto-regressive component to include multiple previous y's. Indeed as the following theorem shows adding sufficiently long auto-regression is powerful enough to capture any LDS.

Theorem 4.1. *Given an LDS parameterized by $A \in \mathbb{R}^{d \times d}, B, C, D$, there exist coefficients $\alpha_{1:d}$ and matrices $\Gamma_{0:d}$ such that given any input sequence $u_{1:L}$, the output sequence $y_{1:L}$ generated by the action of the LDS on the input satisfies for all t*

$$y_t = \sum_{i=1}^{d} \alpha_i y_{t-i} + \sum_{i=0}^{d} \Gamma_i u_{t-i}$$

This is a well-known observation and we provide a proof in Appendix H. Motivated by the above theorem, we propose a generalization of STU, which we call AR-STU. Given a parameter k_y we define AR-STU as

$$\hat{y}_t = \underbrace{\sum_{i=1}^{k_y} \boldsymbol{M_i^y} \hat{y}_{t-i} + \sum_{i=1}^{3} M_i^u u_{t+1-i}}_{\text{Auto-regressive Component}} \tag{8}$$

$$+ \underbrace{\sum_{k=1}^{K} M_k^{\phi+} \sigma_k^{1/4} U_{t-2,k}^{+} + \sum_{k=1}^{K} M_k^{\phi-} \sigma_k^{1/4} U_{t-2,k}^{-}}_{\text{Spectral Component}} . \tag{9}$$

In Table 1, we evaluate the performance of AR-STU on Long Range Arena. In our experiments we search over two values of $k_y = \{2, 32\}$. For non-image tasks, ListOps, Text and Retrieval, we find that setting $k_y = 2$ is sufficient to get optimal results. For the image tasks, CIFAR, Pathfinder and PathX, we found that $k_y = 32$ led to significant performance gains. A performance ablation over this parameter can be found in the appendix (Table 2). Overall we find that the STU model provides improvements over baselines such as S4 and LRU on 4 out of the 6 tasks and performs comparably to the best baseline on the others. Remarkably, the STU layers come with provable guarantees and thus performs well *out of the box* without the need for specific initializations, discretizations or normalizations. We initialize all parameters $M_i^y, M_i^u, M_k^{\phi+}, M_k^{\phi-}$ with 0. We provide details of the experimental setup, including hyperparameter tuning in the appendix (Section G).

5. Conclusion

Inspired by the success of SSMs, we present a new theoretically-founded deep neural network architecture, Spectral SSM, for sequence modelling based on the Spectral Filtering algorithm for learning Linear Dynamical Systems. We demonstrate the core advantages of the Spectal SSM, viz. robustness to long memory through experiments on a synthetic LDS and the Long Range Arena benchmark. We find that the Spectral SSM is able to learn even in the presence of large context lengths/memory without the need for designing specific initializations, discretizations or normalizations which were necessary for existing SSMs to learn in such settings.

References

Blelloch, G. E. Scans as primitive parallel operations. *IEEE Transactions on computers*, 38(11):1526–1538, 1989.

Brown, T., Mann, B., Ryder, N., Subbiah, M., Kaplan, J. D., Dhariwal, P., Neelakantan, A., Shyam, P., Sastry, G., Askell, A., et al. Language models are few-shot learners. *Advances in neural information processing systems*, 33: 1877–1901, 2020.

Dao, T., Fu, D. Y., Saab, K. K., Thomas, A. W., Rudra, A., and Ré, C. Hungry hungry hippos: Towards language modeling with state space models. *arXiv preprint arXiv:2212.14052*, 2022.

Dosovitskiy, A., Beyer, L., Kolesnikov, A., Weissenborn, D., Zhai, X., Unterthiner, T., Dehghani, M., Minderer, M., Heigold, G., Gelly, S., et al. An image is worth 16x16 words: Transformers for image recognition at scale. *arXiv preprint arXiv:2010.11929*, 2020.

Elman, J. L. Finding structure in time. *Cognitive science*, 14(2):179–211, 1990.

Fu, D. Y., Epstein, E. L., Nguyen, E., Thomas, A. W., Zhang, M., Dao, T., Rudra, A., and Ré, C. Simple hardware-efficient long convolutions for sequence modeling. *arXiv preprint arXiv:2302.06646*, 2023.

Gu, A. and Dao, T. Mamba: Linear-time sequence modeling with selective state spaces. *arXiv preprint arXiv:2312.00752*, 2023.

Gu, A., Dao, T., Ermon, S., Rudra, A., and Ré, C. Hippo: Recurrent memory with optimal polynomial projections. In Larochelle, H., Ranzato, M., Hadsell, R., Balcan, M., and Lin, H. (eds.), *Advances in Neural Information Processing Systems*, volume 33, pp. 1474–1487. Curran Associates, Inc., 2020.

Gu, A., Goel, K., and Ré, C. Efficiently modeling long sequences with structured state spaces. *arXiv preprint arXiv:2111.00396*, 2021a.

Gu, A., Johnson, I., Goel, K., Saab, K., Dao, T., Rudra, A., and Ré, C. Combining recurrent, convolutional, and continuous-time models with linear state space layers. *Advances in neural information processing systems*, 34: 572–585, 2021b.

Gupta, A., Gu, A., and Berant, J. Diagonal state spaces are as effective as structured state spaces. In Oh, A. H., Agarwal, A., Belgrave, D., and Cho, K. (eds.), *Advances in Neural Information Processing Systems*, 2022. URL https://openreview.net/forum?id=RjS0j6tsSrf.

Hazan, E., Singh, K., and Zhang, C. Learning linear dynamical systems via spectral filtering. In *Advances in Neural Information Processing Systems*, pp. 6702–6712, 2017.

Hazan, E., Lee, H., Singh, K., Zhang, C., and Zhang, Y. Spectral filtering for general linear dynamical systems. In *Advances in Neural Information Processing Systems*, pp. 4634–4643, 2018.

Hopfield, J. J. Neural networks and physical systems with emergent collective computational abilities. *Proceedings of the national academy of sciences*, 79(8):2554–2558, 1982.

Jumper, J., Evans, R., Pritzel, A., Green, T., Figurnov, M., Ronneberger, O., Tunyasuvunakool, K., Bates, R., Žídek, A., Potapenko, A., et al. Highly accurate protein structure prediction with alphafold. *Nature*, 596(7873):583–589, 2021.

Li, Y., Cai, T., Zhang, Y., Chen, D., and Dey, D. What makes convolutional models great on long sequence modeling? *arXiv preprint arXiv:2210.09298*, 2022.

Orvieto, A., Smith, S. L., Gu, A., Fernando, A., Gulcehre, C., Pascanu, R., and De, S. Resurrecting recurrent neural networks for long sequences. *arXiv preprint arXiv:2303.06349*, 2023.

Poli, M., Massaroli, S., Nguyen, E., Fu, D. Y., Dao, T., Baccus, S., Bengio, Y., Ermon, S., and Ré, C. Hyena hierarchy: Towards larger convolutional language models. *arXiv preprint arXiv:2302.10866*, 2023.

Rumelhart, D. E., Hinton, G. E., Williams, R. J., et al. Learning internal representations by error propagation, 1985.

Shi, J., Wang, K. A., and Fox, E. Sequence modeling with multiresolution convolutional memory. In *International Conference on Machine Learning*, pp. 31312–31327. PMLR, 2023.

Smith, J. T., Warrington, A., and Linderman, S. Simplified state space layers for sequence modeling. In *The Eleventh International Conference on Learning Representations*, 2023.

Tay, Y., Dehghani, M., Abnar, S., Shen, Y., Bahri, D., Pham, P., Rao, J., Yang, L., Ruder, S., and Metzler, D. Long range arena : A benchmark for efficient transformers. In *International Conference on Learning Representations*, 2021. URL https://openreview.net/forum?id=qVyeW-grC2k.

Tay, Y., Dehghani, M., Bahri, D., and Metzler, D. Efficient transformers: A survey. *ACM Comput. Surv.*, 55(6), dec 2022. ISSN 0360-0300. doi: 10.1145/3530811. URL https://doi.org/10.1145/3530811.

Vaswani, A., Shazeer, N., Parmar, N., Uszkoreit, J., Jones, L., Gomez, A. N., Kaiser, Ł., and Polosukhin, I. Attention is all you need. *Advances in neural information processing systems*, 30, 2017.

A. Detailed Related work

State space models. SSMs for learning long range phenomenon have received much attention in the deep learning community in recent years. (Gu et al., 2020) propose the HiPPO framework for continuous-time memorization, and shows that with a special class of system matrices A (HiPPO matrices), SSMs have the capacity for long-range memory. Subsequently, (Gu et al., 2021b) propose the Linear State-Space Layer (LSSL), where the system matrix is learnable. The LSSL can be viewed as a recurrence in the state domain and a convolution in the time domain, and generalizes particular RNN and CNN architectures. For efficient learning of the system matrices, authors propose learning within a class of structured matrices that contain the HiPPO dynamics, and have efficient convolution schemes. However, the proposed method is numerically unstable in practice as well as memory-intensive. As a result, (Gu et al., 2021a) develop the S4 parameterization to address these bottlenecks. The S4 parameterization restricts the system matrices A to be normal plus low-rank, allowing for stable diagonalization of the dynamics. Under this parameterization, authors design memory and computationally efficient methods that are also numerically stable.

The S4 model has been further streamlined in later works. (Gupta et al., 2022) simplify the S4 parameterization to diagonal system matrices, and shows that the diagonal state-space model (DSS) is competitive with S4 on several benchmarks. (Smith et al., 2023) propose the S5 architecture, which improves upon S4 in two directions: 1) instead of having independent SISO SSMs in the feature dimension, S5 has one MIMO DSS that produces vector-valued outputs; 2) S5 uses efficient parallel scans in place of convolutions, bypassing custom-designed algorithms for computing the convolutional filters.

To improve the performance of SSMs on language modeling tasks, (Dao et al., 2022) develops the H3 layer by stacking two SSMs together. They identify two areas where SSMs underperform compared to the transformer: remembering earlier tokens and comparing tokens across the input sequence. The H3 layer includes a shift SSM, where the dynamics matrix is a shifting operator, and a DSS, with multiplicative interactions. The shift SSM enables the layer to store earlier tokens, while the multiplicative interaction allows for comparison (inner product) between tokens in a sequence. They also develop FFT algorithms with better hardware utilization, to close the speed gap between SSMs and Transformers.

Motivated by the similarities between SSMs and RNNs, (Orvieto et al., 2023) investigate whether deep RNNs can recover the performance of deep SSMs, and provide an affirmative answer. The proposed RNN architecture is a deep model with stacked Linear Recurrent Unit (LRU) layers. Each LRU has linear recurrence specified by a complex diagonal matrix, learned with exponential parameterization and proper normalization techniques. The deep LRU architecture has comparable computational efficiency as SSMs and matches their performance on benchmarks that require long-term memory. However, the paper also shows that without the specific modifications on linear RNNS, namely the stable exponential parameterization, gamma normalization and ring initialization, LRU fails to learn on certain challenging long-context modeling tasks. We provide further details about this study after this section.

Spectral filtering. The technique of spectral filtering for learning linear dynamical systems was put forth in (Hazan et al., 2017). This work studies online prediction of the sequence of observations y_t, and the goal is to predict as well as the best symmetric LDS using past inputs and observations. Directly learning the dynamics is a non-convex optimization problem, and spectral filtering is developed as an improper learning technique with an efficient, polynomial-time algorithm and near-optimal regret guarantees. Different from regression-based methods that aim to identify the system dynamics, spectral filtering's guarantee does not depend on the stability of the underlying system, and is the first method to obtain condition number-free regret guarantees for the MIMO setting. Extension to asymmetric dynamical systems was further studied in (Hazan et al., 2018).

Convolutional Models for Sequence Modeling Exploiting the connnection between Linear dynamical systems and convolutions (as highlighted by (Gu et al., 2021a)) various convolutional models have been proposed for sequence modelling. (Fu et al., 2023) employ direct learning of convolutional kernels directly to sequence modelling but find that they underperform SSMs. They find the non-smoothness of kernels to be the culprit and propose applying explicit smoothing and squashing operations to the kernels to match performance on the Long Range Arena benchmark. The proposed model still contains significantly large number of parameters growing with the sequence length. (Li et al., 2022) identifies two key characteristics of convolutions to be crucial for long range modelling, decay in filters and small number of parameters parameterizing the kernel. They achieve this via a specific form of the kernel derived by repeating and scaling the kernel in a dyadic fashion. (Shi et al., 2023) propose a multiresolution kernel structure inspired from the wavelet transform and multiresolution analysis.

All these methods parameterize the kernels with specific structures and/or add further regularizations to emulate the convolution kernels implied by SSMs. In contrast our proposed kernels are *fixed and thereby parameter-free* and the number of parameters scale in the number of kernels and not the size of the kernel. Furthermore our kernels are *provably more expressive* than linear dynamical systems capable of directly capturing and improving the performance of SSMs without the need for specific initializations. Naturally our kernels (see Fig **??**) by default satisfy both the smoothness and the decay condition identified (and explicitly enforced) by (Li et al., 2022) and (Fu et al., 2023).

A.1. Ablations performed by (Orvieto et al., 2023)

Motivated by the success of SSMs, (Orvieto et al., 2023) revisit the RNN model (under the same deep stacked structure as SSMs) to investigate their efficiency. They begin from a simple linear RNN (a directly parameterized LDS) and add multiple components inspired from the SSM literature to ensure numerical stability and trainability of the model especially as the sequences grow larger. Overall they demonstrate that carefully designed parameterizations and initializations of LDS parameters as well as specifically designed normalizations are all necessary for model to learn consistently over the LRA dataset and in particularly over the 16K context length task PathX. These interventions are driven by specific intuitions such as an inductive bias towards larger memory or controlling the loss blowup at initialization under long contexts but as such come with no theoretical guarantees towards alleviating the problem. We provide some quick details towards what these interventions are and refer the reader to (Orvieto et al., 2023) to understand the motivations behind them and comparisons with similar ideas existing in previous SSM literature. The LRU model considered by (Orvieto et al., 2023) is given by

$$y_k = \text{diag}(\lambda) y_{k-1} + \gamma \odot B u_k.$$

In the above the learned parameters are λ and B and note that $\text{diag}(\lambda)$ corresponds to a diagonal A. γ is a specific normalization technique they develop to control the loss blowup under long-context detailed below. They perform the following interventions towards stable training

- **Stable Exponential Parameterization**: They parameterize λ as

  $$\lambda_j = \underbrace{\exp(-\exp(\nu_j^{\log})}_{\text{magnitude}} + i \underbrace{\exp(\theta_j^{\log})}_{\text{phase}})$$

  The above is done to ensure a bound on the magnitude of eigenvalues of the effective A matrix as well as to ensure more *resolution* in the parameter space closer to the value of 1.

- **Ring Initialization**: They initialize the λ_j in the complex annulus $[\text{min\_rad}, \text{max\_rad}]$. This ensures that at initialization the magnitude of λ_j chosen randomly lies in $\in [\text{min\_rad}, \text{max\_rad}]$ and the phase is chosen randomly. When not applying this intervention min_rad and max_rad are chosen to be 0,1 respectively. When applying this intervention these values are chosen to be closer to 1, e.g. $0.9, 0.999$ respectively.

- **γ-Normalization**: They set $\gamma_j = \sqrt{1 - |\lambda_j|^2}$

- **Restricting Phase at initialization**: Instead of drawing a random phase at initialization the authors recommend selecting the initial phase from $[0, \pi/10]$. The authors claim that uniform phase inherently biases the network towards learning spurious features in the input sequence.

(Orvieto et al., 2023) provide the following ablation in the paper. In particular we see that all the above interventions are necessary to make the model get to non-trivial accuracy on PathX. On the contrary, as we show the STU model achieves comparable accuracy without requiring any specific initialization or normalization.

Model	Specification	sCIFAR	ListOps	Pathfinder	PathX
LRU	Dense A	72.2	50.4	✗	✗
	Λ Exp. Param.	85.4	60.5	65.4	✗
	Λ Stable Exp. Param.	87.2	59.4	93.5	✗
	+ Ring Init.	88.1	59.4	94.4	✗
	+ γ-Norm. + Phase Init.	89.0	60.2	95.1	94.2

B. Preliminaries

Sequence prediction. We treat sequence prediction as a game between a predictor/learner and nature in which iteratively at every time $t \in [L]$, the learner is presented an input $u_t \in \mathbb{R}^{d_{\text{in}}}$. The learner A then produces a candidate output $\hat{y}_t = \hat{y}_t(A)$, and nature reveals the t^{th} element of a target sequence $y_t \in \mathbb{R}^{d_{\text{out}}}$. The learner then suffers an instantaneous loss of $\|y_t - \hat{y}_t\|^2$. The task of the learner is to minimize regret over a benchmark set of learning algorithms $\mathcal{A}$, defined as follows

$$\text{Regret} = \sum_{t=1}^{L} \|y_t - \hat{y}_t\|^2 - \min_{A \in \mathcal{A}} \sum_{t=1}^{L} \|y_t - \hat{y}_t(A)\|^2.$$

Linear Dynamical Systems (LDS): An example benchmark set of methods is that of a linear dynamical system, which has four matrix parameters, $A \in \mathbb{R}^{N \times N}, B \in \mathbb{R}^{N \times d_{\text{in}}}, C \in \mathbb{R}^{d_{\text{out}} \times N}, D \in \mathbb{R}^{d_{\text{out}} \times d_{\text{in}}}$. The system evolves and generates outputs according to the following equations

$$x_t \triangleq Ax_{t-1} + Bu_t, \qquad \hat{y}_t \triangleq Cx_t + Du_t \tag{10}$$

Thus, an example class of benchmark algorithms $\mathcal{A}$ are all predictors that generate $\hat{y}_t$ according to these rules, for a fixed set of matrices A, B, C, D.

Spectral Filtering: Another important set of predictors is one which is inspired by spectral filtering (Hazan et al., 2017). The spectral filtering theory builds an efficient representation for all vectors in the range of the function $\mu : [0, 1] \to \mathbb{R}^L$ defined as $\mu(\alpha) \triangleq (\alpha - 1)[1, \alpha, \alpha^2 \ldots]$. To build this representation, for any L define the following Hankel matrix $Z \in \mathbb{R}^{L \times L}$ whose entries are given by

$$Z[i, j] \triangleq \frac{2}{(i + j)^3 - (i + j)}$$

It is shown in the appendix (see Lemma E.1) that $Z = \int_0^1 \mu(\alpha)\mu(\alpha)^\top d\alpha$. Thus it can be seen that Z is a real PSD Hankel matrix. It is known (see Lemma E.4 in the appendix) that real PSD Hankel matrices have an exponentially decaying spectrum. As a result, the crux of the spectral filtering theory, lies in showing that for all $\alpha \in [0, 1]$ [3], the vector $\mu(\alpha)$ is approximately contained in the subspace spanned by the top eigenvectors of Z, making the subspace spanned by top-eigenvectors of Z a very efficient subspace to project the input into. This fact is formalized as Lemma E.3 in the appendix. We now use this intuition to describe the Spectral Filtering algorithm.

Since Z is a real PSD matrix, it admits a real spectral decomposition, and the (non-negative) eigenvalues can be easily ordered naturally by their value. Let $\{(\sigma_j \in \mathbb{R}, \phi_j \in \mathbb{R}^T)\}_{j=1}^{L}$ be the eigenvalue-eigenvector pairs of Z ordered to satisfy $\sigma_1 \geq \sigma_2 \geq \ldots \geq \sigma_d$. We consider a fixed number K of the above eigenvectors. Algorithms in the spectral filtering class generate $\hat{y}_t$ as follows. For each $k \in K$, we first featurize the input sequence by *projecting* the input sequence until time t on ϕ_k, leading to a sequence $U_{t,k} \in \mathbb{R}^{d_{\text{in}}}$ defined as

$$U_{t,k} = \sum_{i=1}^{t} u_{t-i} \cdot \phi_k(i).$$

[3] in particular all α close to 1, representing marginally stable systems.

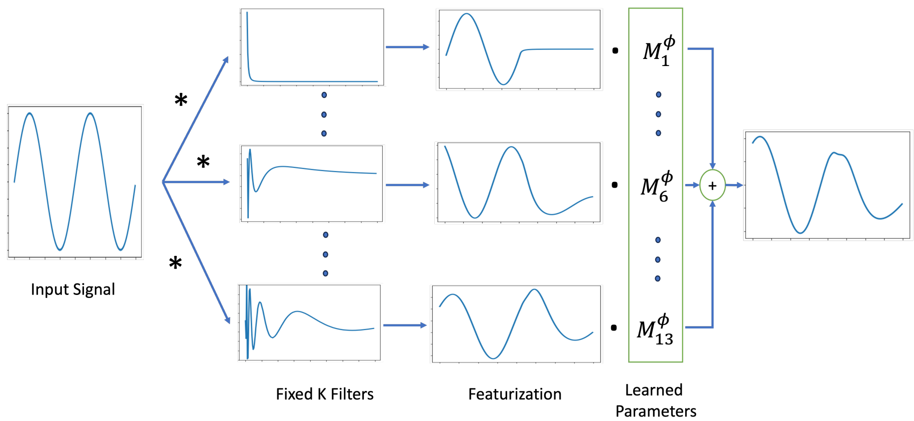

Figure 2: Schematic showing the spectral projection of a 1-dimensional input sequence and how these features are used to produce the spectral component in the STU output (5). In the multi-dimensional case the operation is applied in parallel across every input dimension.

The spectral filtering class is further parameterized by matrices $M_1^u \in \mathbb{R}^{d_{\text{out}} \times d_{\text{in}}}$, $M_2^u \in \mathbb{R}^{d_{\text{out}} \times d_{\text{in}}}$ and a set of matrices $M_1^\phi, ..., M_K^\phi \in \mathbb{R}^{d_{\text{out}} \times d_{\text{in}}}$. The output at time t is then given by

$$\hat{y}_t = \hat{y}_{t-1} + M_1^u u_t + M_2^u u_{t-1} + \sum_{k=1}^{K} M_k^\phi U_{t,k}. \tag{11}$$

Note that given an input sequence $u_{1:L}$ for any k, the $d_{\text{in}} \times T$ matrix $U_{1:L,k}$ can be efficiently computed via convolutions along the time dimension L in total time $O(d_{\text{in}} \cdot L \log(L))$. The following theorem (proved in (Hazan et al., 2017)) establishes that the spectral filtering class of predictors approximately contains bounded linear dynamical systems with positive semi-definite A.

Theorem B.1. *Given any A, B, C, D such that A is a PSD matrix with $\|A\| \leq 1$ and given any numbers $K \in \mathbb{I}^+, a \in \mathbb{R}^+$, there exists matrices $M_1^u, M_2^u, M_1^\phi, ..., M_K^\phi$, such that for all L and all sequences $u_{1:L}$ satisfying $\|u_t\| \leq a$ for all $t \in [L]$ the following holds. Let $y_{1:L}^{\text{LDS}}$ be the sequence generated by execution of the LDS given by A, B, C, D (via (10)) and $y_{1:L}^{\text{SF}}$ be the sequence generated by Spectral Filtering (via (3)) using the matrices $M_1^u, M_2^u, M_1^\phi, ..., M_K^\phi$. Then for all $t \in [L]$,*

$$\|y_t^{\text{LDS}} - y_t^{\text{SF}}\|^2 \leq c \cdot \|B\|_{col} \cdot \|C\|_{col} \cdot L^3 \cdot a \cdot e^{-\left(\frac{\pi^2}{4} \cdot \frac{K}{\log(L)}\right)}$$

where $c \leq 10^6$ is a universal constant and $\|B\|_{col}$, $\|C\|_{col}$ are the maximum column norm of the matrices B and C respectively.

We do not provide a proof for this theorem which can be found in (Hazan et al., 2017) [4]. Instead, in the next section we provide a generalization of this theory to cover all symmetric matrices and not just PSD matrices and prove a more general theorem (Theorem 2.1). We further build upon this generalization to create a sequence to sequence prediction unit.

C. Learning a marginally-stable LDS

We provide a simple synthetic evaluation of the stability and training efficiency afforded by the STU. We consider a low-dimensional linear system A, B, C, D generated as follows. $B \in \mathbb{R}^{4\times3}, C \in \mathbb{R}^{3\times4}$ are matrices with iid unit Gaussian entries. D is a diagonal matrix with iid unit Gaussian entries and A is a diagonal matrix with $A_{ii} \sim 0.9999 * Z$ where Z is a random sign. By design this is a system with a very high stability constant ($\sim 10^4$). As a training dataset we generated $\{(u_i, y_i)\}$ where u_i is a random input sequence and y_i is the output generated by applying the linear dynamical system on u_i. We perform mini-batch (batch size 1) training with the l2 loss. As comparison we perform the same procedure with an

[4] Note that (Hazan et al., 2017) consider a simpler setting where in the ground truth y_t is available to the learner for all future time steps. We do not make such an assumption and theorems have been adjusted to suffer an additional L factor in the error as a result.

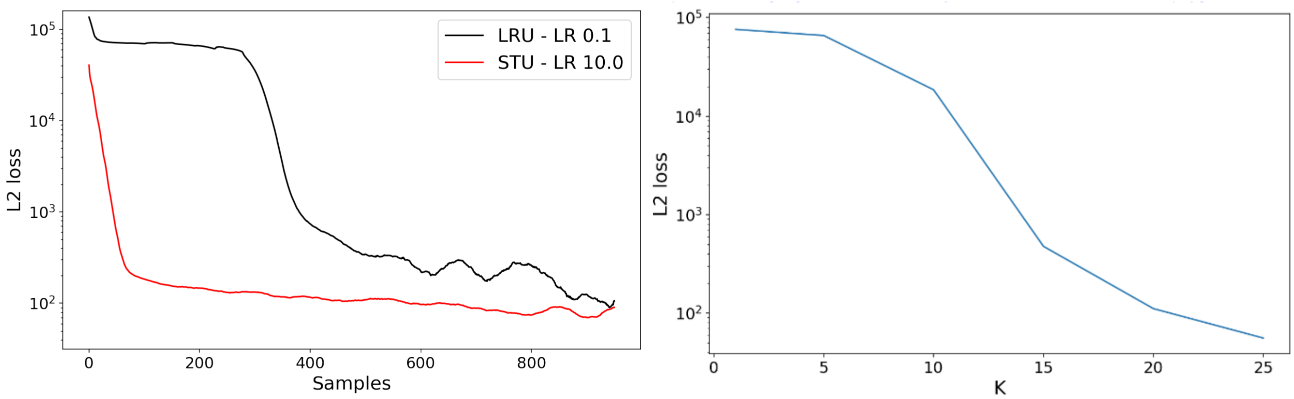

(a) (b)

Figure 3: Learning dynamics for learning a marginally stable LDS. (a.)(Smoothed) Learning curves for a single STU layer (red) vs a single LRU layer (black). The learning rate was tuned for both models. See Appendix for a detailed discussion of the tuning and sensitivity to hyperparameters for both the models. Curiously at stable LRs we observe that LRUs show a plateauing of learning. (b.) Error (in log-scale) obtained by the single STU layer as a function of the model parameter 'K'. We observe an exponential drop in the reconstruction loss as predicted by the analysis.

LRU (Linear Recurrent Unit) layer as proposed by (Orvieto et al., 2023) which directly parameterizes the linear system. The results of the training loss as seen by the two systems are presented in Figure 3a.

We use all the initialization/normalization techniques as recommended by (Orvieto et al., 2023) for LRU including the *stable exponential parameterization*, *γ-normalization* and *ring-initialization*. Indeed we find that all these tricks were necessary to learn this system at all. We provide more details about the ablations and other hyperparameter setups in the appendix. We observe that the STU is significantly more efficient at learning the LDS as opposed to the LRU. We further find that there is a wide range of LRs where the STU has a stable optimization trajectory and the loss decreases continuously highlighting the advantages of a convex parameterization. On the other hand, LRU is able to eventually learn the system at the right learning rates, it requires almost 8x the number of samples to get to a system with non-trivial accuracy. More details can be found in the appendix. Curiously we observe that for the LRU training plateaus completely for the first 50% of training highlighting the difficulty of optimization via a non-convex landscape.

The STU layer in the previous experiment employs $K = 25$. In Figure 3b we plot the performance of STU at various levels of K. As predicted by the theory we observe an exponential decay in the error as K increases with the error effectively plateauing after $K \geq 15$.

D. Computational complexity and comparison to other methods.

Using the STU method to make a sequence of L predictions, the features $U^+, U^- \in \mathbb{R}^{L \times d_{\text{in}} \times K}$ can be computed in time $O(K \cdot L \cdot d_{\text{in}} \log(L))$ using the Discrete Fast Fourier Transform, where K is the number of filters and L is the context length. The linear prediction part (i.e. spectral component) takes $O(K \cdot L \cdot d_{\text{in}} \cdot d_{\text{out}})$ time, and the autoregressive part can be implemented in total time $O(L \cdot d_{\text{in}} \cdot d_{\text{out}})$. Therefore the overall runtime is $O(K \cdot L \cdot d_{\text{in}} \cdot (\log(L) + d_{\text{out}}))$. [5]

For comparison, consider LRU and transformers. The same computation carried out by LRU w. diagonal system matrices is dominated by the hidden dimension, i.e. $O(L \cdot d_{\text{hidden}} \cdot (d_{\text{in}} + d_{\text{out}}))$. Thus, the number of filters is replaced by d_{hidden}, which is usually an order of magnitude larger, although STU has another $O(\log L)$ overhead.

A transformer model with full attention runs in time $O(L^2 d_{\text{in}} d_{\text{out}})$, which is significantly more costly than both LRU and STU. This is consistent with the motivation of SSM as more efficient models for sequences.

[5] We shortly note that the K filters can be distributed amongst K machines and their computations done separately. There are many other opportunities for distributed computing for all architectures which we will not survey here as it is out of scope.

E. Proof of Theorem 2.1

We begin by observing that without loss of generality we can assume that A is a real-diagonal matrix. This can be ensured by performing a spectral decomposition of $A = U\Sigma U^\top$ and *absorbing* the $U, U^\top$ by redefining the system. Before continuing with the proof, we will provide some requisite definitions and lemmas. Define the following vector for any $\alpha \in \mathbb{R}$, $\mu(\alpha) \in \mathbb{R}^L$, with $\mu(\alpha)(i) = (\alpha - 1)\alpha^{i-1}$. Further define the Hankel matrix H as

$$Z \triangleq \int_0^1 \mu(\alpha)\mu(\alpha)^\top d\alpha.$$

As the following lemma shows the Hankel matrix Z above is the same Hankel matrix defined in the definition of STU (2).

Lemma E.1. *Z is a Hankel matrix with entries given as*

$$Z(i,j) = \frac{2}{(i+j)^3 - (i+j)}$$

Lemma E.2. *We have that the following statements hold regarding $\mu(\alpha)$ for any $\alpha \in [0,1]$,*

- $|\mu(\alpha)|^2 \leq 1$
- *For any $\alpha \in [0,1]$ and any unit vector v we have that*

$$(\mu(\alpha)^\top v)^2 \leq 12(v^\top H v)$$

Lemma E.3. *For any $\alpha \in [0,1]$, let $\tilde{\mu}(\alpha)$ be the projection of $\mu(\alpha)$ on the subspace spanned by top k eigenvectors of Z, then we have that*

$$\|\mu(\alpha) - \tilde{\mu}(\alpha)\|^2 \leq 12 \sum_{i=k+1}^{L} \sigma_i$$

Finally the following lemma from (Hazan et al., 2017) shows that the spectrum of the matrix Z decays exponentially.

Lemma E.4 (Lemma E.3 (Hazan et al., 2017))**.** *Let σ_j be the top j^{th} eigenvalue of Z. Then we have that*

$$\sigma_j \leq \Gamma c^{-j/\log(L)}$$

where $c = e^{\pi^2/4} \sim 11.79$ and $\Gamma = 235200$ is an absolute constant.

We now move towards proving Theorem 2.1. Consider the following calculation for the LDS sequence y_t^{LDS}

$$y_t^{\mathrm{LDS}} = \sum_{i=0}^{T} CA^i B u_{t-i} + Du_t,$$

and therefore we have that

$$y_t^{\mathrm{LDS}} - y_{t-2}^{\mathrm{LDS}} = (CB + D)u_t + CABu_{t-1} - Du_{t-2} + \underbrace{\sum_{i=0}^{T} C(A^{i+2} - A^i)Bu_{t-2-i}}_{\text{Term of Interest}}$$

For any $t_1 \geq t_2$ we define the matrix $\bar{U}_{\{t_1:t_2\}} \in \mathbb{R}^{d_{\mathrm{out}} \times t_1 - t_2 + 1}$ whose i^{th} column is the input vector $u_{t_1 - i + 1}$. We allow t_2 to be negative and by convention assume $u_t = 0$ for any $t \leq 0$. Denote the diagonal entries of A by $\{\alpha_l\}_{l=1}^{d_h}$, i.e. $\alpha_l = A(l,l)$. Further let b_l, c_l be the l-th column for the matrices B, C respectively. The term of interest above can then be written as

$$\begin{aligned}
&\sum_{i=0}^{L} C(A^{i+2} - A^i) B u_{t-2-i} \\
&= \sum_{l=1}^{d_h} (c_l \otimes b_l) \left(\sum_{i=0}^{L} (\alpha_l^{i+2} - \alpha_l^i) u_{t-2-i} \right) \\
&= \sum_{l:\alpha_l \geq 0} (c_l \otimes b_l) \left(\sum_{i=0}^{L} (\alpha_l^2 - 1)\alpha_l^i u_{t-2-i} \right) + \sum_{l:\alpha_l < 0} (c_l \otimes b_l) \left(\sum_{i=0}^{L} (\alpha_l^2 - 1)\alpha_l^i u_{t-2-i} \right) \\
&= \sum_{l:\alpha_l \geq 0} (\alpha_l + 1)(c_l \otimes b_l) \left(\sum_{i=0}^{L} (\alpha_l - 1)\alpha_l^i u_{t-2-i} \right) + \sum_{l:\alpha_l < 0} (1 + |\alpha_l|)(c_l \otimes b_l) \left(\sum_{i=0}^{L} (|\alpha_l| - 1)|\alpha_l|^i (-1)^i u_{t-2-i} \right) \\
&= \sum_{l:\alpha_l \geq 0} (\alpha_l + 1)(c_l \otimes b_l) \left(\bar{U}_{\{t-2:t-1-L\}} \mu(\alpha) \right) + \sum_{l:\alpha_l < 0} (|\alpha_l| + 1)(c_l \otimes b_l) \left(\bar{U}_{\{t-2:t-1-L\}} \odot \mathbf{1}^{\pm} \right) \mu(|\alpha_l|)
\end{aligned}$$

where $\mathbf{1}^{\pm} \in \mathbb{R}^{d_{\text{out}} \times L}$ is defined as the matrix whose every row is the alternating sign vector $[1, -1, 1, -1 \ldots])$ and $\odot$ is Hadamard product (i.e. entry-wise multiplication).

$$\begin{aligned}
y_t^{\text{LDS}} - y_{t-2}^{\text{LDS}} = (CB + D)u_t + CABu_{t-1} - Du_{t-2} + \underbrace{\sum_{l:\alpha_l \geq 0} (\alpha_l + 1)(c_l \otimes b_l) \left(\bar{U}_{\{t-2:t-1-L\}} \mu(\alpha) \right)}_{PositivePart} \\
+ \underbrace{\sum_{l:\alpha_l < 0} (|\alpha_l| + 1)(c_l \otimes b_l) \left(\bar{U}_{\{t-2:t-1-L\}} \odot \mathbf{1}^{\pm} \right) \mu(|\alpha_l|)}_{NegativePart}
\end{aligned} \tag{12}$$

Recall that we defined the sequence $\{\sigma_k, \phi_k\}_{k=1}^{L}$ to be the eigenvalue and eigenvector pairs for the Hankel matrix Z. For any α we define the projection of $\mu(\alpha)$ on the top k eigenvectors as $\tilde{\mu}(\alpha)$, i.e. $\tilde{\mu}(\alpha) = \sum_{k=1}^{K} (\mu(\alpha_l)^\top \phi_k)\phi_k$. Further define STU parameters as follows

$$\begin{aligned}
M_1^u &= CB + D, M_2^u = CAB, M_3^u = -D \\
M_k^{\phi+} &= \sum_{l:\alpha_l \geq 0} (\alpha_l + 1)(\mu(\alpha_l)^\top \phi_k)\sigma_k^{-1/4}(c_l \otimes b_l) \\
M_k^{\phi-} &= \sum_{l:\alpha_l < 0} (|\alpha_l| + 1)(\mu(|\alpha_l|)^\top \phi_k)\sigma_k^{-1/4}(c_l \otimes b_l)
\end{aligned} \tag{13}$$

By the definition of STU prediction (5) we have that,

$$\begin{aligned}
y_t^{\text{STU}} &= y_{t-2}^{\text{STU}} + \sum_{i=1}^{3} M_i^u u_{t+1-i} + \sum_{k=1}^{K} M_k^{\phi+} \sigma_k^{1/4} \left(\sum_{i=0}^{t-1} u_{t-i} \cdot \phi_k(i) \right) + \sum_{k=1}^{K} M_k^{\phi-} \sigma_k^{1/4} \left(\sum_{i=0}^{t-1} u_{t-i} \cdot (-1)^i \cdot \phi_k(i) \right) \\
&= y_{t-2}^{\text{STU}} + \sum_{i=1}^{3} M_i^u u_{t+1-i} + \sum_{k=1}^{K} M_k^{\phi+} \sigma_k^{1/4} \left(\bar{U}_{\{t-2:t-1-L\}} \phi_k \right) + \sum_{k=1}^{K} M_k^{\phi-} \sigma_k^{1/4} \left((\bar{U}_{\{t-2:t-1-L\}} \odot \mathbf{1}^{\pm})\phi_k \right).
\end{aligned}$$

Using the parameters specified in (13) in the above we have that,

$$y_t^{\mathrm{STU}} - y_{t-2}^{\mathrm{STU}} = (CB + D)u_t + CABu_{t-1} - Du_{t-2} + \sum_{l:\alpha_l \geq 0} (\alpha_l + 1)(c_l \otimes b_l) \left(\bar{U}_{\{t-2:t-1-L\}}\right) \left(\underbrace{\sum_{k=1}^{K} (\mu(\alpha_l)^\top \phi_k)\phi_k}_{=\tilde{\mu}(\alpha)} \right)$$

$$+ \sum_{l:\alpha_l < 0} (|\alpha_l| + 1)(c_l \otimes b_l) \left(\bar{U}_{\{t-2:t-1-L\}} \odot \mathbf{1}^{\pm}\right) \left(\underbrace{\sum_{k=1}^{K} (\mu(|\alpha_l|)^\top \phi_k)\phi_k}_{=\tilde{\mu}(|\alpha_l|)} \right)$$

Combining the above display with (12), we get that

$$\begin{aligned} y_t^{\mathrm{LDS}} - y_t^{\mathrm{STU}} = y_{t-2}^{\mathrm{LDS}} - y_{t-2}^{\mathrm{STU}} &+ \sum_{l:\alpha_l \geq 0} (\alpha_l + 1)(c_l \otimes b_l) \left(\bar{U}_{\{t-2:t-1-L\}}\right) (\mu(\alpha) - \tilde{\mu}(\alpha)) \\ &+ \sum_{l:\alpha_l < 0} (|\alpha_l| + 1)(c_l \otimes b_l) \left(\bar{U}_{\{t-2:t-1-L\}} \odot \mathbf{1}^{\pm}\right) (\mu(|\alpha_l|) - \tilde{\mu}(|\alpha_l|)) \end{aligned} \tag{14}$$

Let $\|B\|_{\text{col}} = \max_l \|b_l\|$, $\|C\|_{\text{col}} = \max_l \|c_l\|$ be the maximum column norms of B and C respectively. Therefore we have that for all l, the spectral norm of the matrix $c_l \otimes b_l$ is bounded as $\|B\|_{\text{col}} \cdot \|C\|_{\text{col}}$. Further note that every column of $\bar{U}$ is an input u_t for some time t. Further we have assumed that $\|u_t\| \leq a$ for all t. Therefore we have that the frobenius norm (and thus spectral norm) of $U_{t-2:t-1-L}$ is bounded as

$$\|\bar{U}_{t-2:t-1-L}\| \leq \|\bar{U}_{t-2:t-1-L}\|_F \leq \sqrt{L} \cdot a.$$

Putting the above together we get that for all l,

$$\|(\alpha_l + 1)(c_l \otimes b_l) \left(\bar{U}_{t-2:t-1-L}\right)\| \leq |(\alpha_l + 1)| \|(c_l \otimes b_l)\| \| \left(\bar{U}_{t-2:t-1-L}\right)\| \leq 2 \cdot \|B\|_{\text{col}} \cdot \|C\|_{\text{col}} \cdot \sqrt{L} \cdot a.$$

Therefore we have (using E.3 that,

$$\begin{aligned} &\| \sum_{l:\alpha_l \geq 0} (\alpha_l + 1)(c_l \otimes b_l) \left(\bar{U}_{t-2:t-1-L}\right) (\mu(\alpha) - \tilde{\mu}(\alpha)) \| \\ &\leq \sum_{l:\alpha_l \geq 0} \|(\alpha_l + 1)(c_l \otimes b_l) \left(\bar{U}_{t-2:t-1-L}\right)\| \cdot \| (\mu(\alpha) - \tilde{\mu}(\alpha)) \| \\ &\leq 5 \cdot \|B\|_{\text{col}} \cdot \|C\|_{\text{col}} \cdot L^{1.5} \cdot a \cdot \sqrt{\sum_{i=K+1}^{L} \sigma_i}. \end{aligned}$$

Similarly we have that

$$\| \sum_{l:\alpha_l < 0} (|\alpha_l| + 1)(c_l \otimes b_l) \left(\bar{U}_{\{t-2:t-1-L\}} \odot \mathbf{1}^{\pm}\right) (\mu(|\alpha_l|) - \tilde{\mu}(|\alpha_l|)) \| \leq 5 \cdot \|B\|_{\text{col}} \cdot \|C\|_{\text{col}} \cdot L^{1.5} \cdot a \cdot \sqrt{\sum_{i=K+1}^{L} \sigma_i}.$$

Plugging the above into (14), we get that

$$\|y_t^{\mathrm{LDS}} - y_t^{\mathrm{STU}}\| \leq \|y_{t-2}^{\mathrm{LDS}} - y_{t-2}^{\mathrm{STU}}\| + 10 \cdot \|B\|_{\text{col}} \cdot \|C\|_{\text{col}} \cdot L^{1.5} \cdot a \cdot \sqrt{\sum_{i=K+1}^{L} \sigma_i}$$

Applying the above equation recursively and Lemma E.4 we get that for any $K \geq \log(L)$,

$$\|y_t^{\text{LDS}} - y_t^{\text{STU}}\| \leq 5 \cdot \|B\|_{\text{col}} \cdot \|C\|_{\text{col}} \cdot L^{2.5} \cdot a \cdot \sqrt{\sum_{i=K+1}^{L} \sigma_i} \leq c \cdot \|B\|_{\text{col}} \cdot \|C\|_{\text{col}} \cdot L^3 \cdot a \cdot e^{\left(-\frac{\pi^2}{4} \cdot \frac{K}{\log(L)}\right)}.$$

where $c = 5\Gamma \leq 2 \times 10^6$ is an absolute constant. This finishes the proof of the theorem.

E.1. Proofs of Lemmas

Proof of Lemma E.1. The lemma follows from the following simple calculations.

$$\begin{aligned} Z(i,j) = \int_0^1 (\alpha-1)^2 \alpha^{i+j-2} d\alpha &= \int_0^1 \left(\alpha^{i+j} + \alpha^{i+j-2} - 2\alpha^{i+j-1}\right) d\alpha \\ &= \frac{1}{(i+j+1)} + \frac{1}{(i+j-1)} - \frac{2}{(i+j)} \\ &= \frac{2}{(i+j)^3 - (i+j)} \end{aligned}$$

□

Lemma E.3 is immediate from the second part of Lemma E.2. We show Lemma E.2 below.

Proof of Lemma E.2. By definition $\mu(\alpha) = 0$ for $\alpha \in \{0,1\}$. Otherwise we have that for all $\alpha \in (0,1)$,

$$|\mu(\alpha)|^2 = \sum_{i=1}^{T} (\alpha-1)^2 \alpha^{2i-2} \leq \frac{(\alpha-1)^2}{(1-\alpha^2)} \leq \frac{1-\alpha}{1+\alpha} \leq 1-\alpha$$

To prove the second part we consider drawing α from the uniform distribution between $[0,1]$. We get that

$$E[(\mu(\alpha)^\top v)^2] = v^\top Z v$$

We now show that the worst case value is not significantly larger than the expectation. To this end we consider the function $f(\alpha) = (\mu(\alpha)^\top v)^2$ and we show that this is a 6-Lipschitz function. To this end consider the following,

$$\begin{aligned} \left\|\frac{\partial \mu(\alpha)}{\partial \alpha}\right\|_2^2 &= \sum_{i=0}^{T-1} \left\{ \left| \frac{\partial}{\partial \alpha} (1-\alpha)\alpha^i \right|^2 \right\} \\ &= \sum_{i=0}^{T-1} \left((1-\alpha) i \alpha^{i-1} - \alpha^i\right)^2 \\ &\leq 2(1-\alpha)^2 \sum_{i=1}^{T-1} i^2 \alpha^{2(i-1)} + 2\sum_{i=0}^{T-1} \alpha^{2i} && (a+b)^2 \leq 2(a^2+b^2) \\ &\leq 2(1-\alpha)^2 \left(\frac{1}{(1-\alpha^2)^2} + \frac{2\alpha^2}{(1-\alpha^2)^3}\right) + \frac{2}{1-\alpha^2} && \sum_{i=1}^{\infty} i^2 \beta^{i-1} = \frac{1}{(1-\beta)^2} + \frac{2\beta}{(1-\beta)^3} \\ &= \frac{2}{(1+\alpha)^2} + \frac{4\alpha^2}{(1-\alpha^2)(1+\alpha)^2} + \frac{2}{1-\alpha^2}. \end{aligned}$$

Therefore we have that for all $\alpha \in [0,1]$,

$$\begin{aligned} \frac{\partial f(\alpha)}{\partial \alpha} = 2(\mu(\alpha)^\top v) \left(\frac{\partial \mu(\alpha)^\top}{\partial \alpha} v\right) &\leq 2\|\mu(\alpha)\|\|v\|^2 \|\frac{\partial \mu(\alpha)}{\partial \alpha}\| \\ &\leq 2\sqrt{(1-\alpha) * \left(\frac{2}{(1+\alpha)^2} + \frac{4\alpha^2}{(1-\alpha^2)(1+\alpha)^2} + \frac{2}{1-\alpha^2}\right)} \\ &\leq 2\sqrt{\left(\frac{2(1-\alpha)}{(1+\alpha)^2} + \frac{4\alpha^2}{(1+\alpha)^3} + \frac{2}{1+\alpha}\right)} \leq 6. \end{aligned}$$

Now for the positive function $f(\alpha)$ which is 6-Lipschitz on $[0, 1]$ let the maximum value be R. It can be seen the lowest expected value of $f(\alpha)$ over the uniform distribution over $[0, 1]$, one can achieve is $R^2/2 * 6$ and therefore we have that

$$R^2/12 \leq v^\top Z v \Rightarrow R \leq \sqrt{12 v^\top H v},$$

which finishes the proof.

□

F. Alternative Representation for capturing negative eigenvalues

In this section we setup an alternative version of STU wherein a different Hankel matrix is used but one can get a similar result. As before a single layer of STU (depicted in figure 2) is parameterized by a number K, denoting the number of eigenfactors and matrices $M_1^\phi \dots M_K^\phi \in \mathbb{R}^{d_{\text{out}} \times d_{\text{in}}}$, and $M_1^u, M_2^u, M_3^u \in \mathbb{R}^{d_{\text{out}} \times d_{\text{in}}}$. The matrices form the *params* of the layer. We use a different Hankel matrix $Z_L \in \mathbb{R}^{L \times L}$ whose entries are given by

$$Z_L[i, j] \triangleq ((-1)^{i+j-2} + 1) \cdot \frac{8}{(i + j + 3)(i + j - 1)(i + j + 1)}. \tag{15}$$

and let $\{(\sigma_j \in \mathbb{R}, \phi_j \in \mathbb{R}^T)\}_{j=1}^T$ be the eigenvalue-eigenvector pairs of Z_L ordered to satisfy $\sigma_1 \geq \sigma_2 \dots \sigma_d$.

Given an input sequence $\{u_1 \dots u_L\} \in \mathbb{R}^{d_{\text{in}}}$, as before we first featurize the input sequence by *projecting* the input sequence till time t on *fixed* filters ϕ_k. The main difference is that we do not need to create a negative featurization now. We define

$$U_{t,k} = \sum_{i=0}^{t-1} u_{t-i} \cdot \phi_k(i).$$

Note that for every k, the sequence of features $X_{1:T,k}$ can be computed efficiently via convolution. The output sequence $\{y_1 \cdots y_T\}$ is then given by

$$\hat{y}_t = \underbrace{\hat{y}_{t-2} + \sum_{i=1}^{3} M_i^u u_{t+1-i}}_{\text{Auto-regressive Component}} + \underbrace{\sum_{k=1}^{K} M_k^\phi \sigma_k^{1/4} X_{t-2,k}}_{\text{Spectral Component}}. \tag{16}$$

We prove the following representation theorem which shows that the above class approximately contains any marginally-stable LDS with symmetric A.

Theorem F.1. *Given any A, B, C, D such that A is a symmetric matrix with $\|A\| \leq 1$ and given any numbers $K \in \mathbb{I}^+, a \in \mathbb{R}^+$, there exists matrices $M_1^u, M_2^u, M_3^u, M_1^\phi \dots M_K^\phi \in \mathbb{R}^{d_{\text{out}} \times d_{\text{in}}}$ for all L and all sequences $u_{1:L}$ satisfying $\|u_t\| \leq a$ for all $t \in [L]$ the following holds. Let $y_{1:L}^{\text{LDS}}$ be the sequence generated by execution of the LDS given by A, B, C, D (via (10)) and $y_{1:L}^{\text{SF}}$ be the sequence generated by Spectral Filtering (via (16)) using the matrices $M_1^u, M_2^u, M_3^u, M_1^{\phi+} \dots M_K^{\phi+}, M_1^{\phi-} \dots M_K^{\phi-}$. Then for all $t \in [T]$, we have that*

$$\|y_t^{\text{LDS}} - y_t^{\text{SF}}\|^2 \leq c \cdot \|B\|_{col} \cdot \|C\|_{col} \cdot L^3 \cdot a \cdot e^{-\left(\frac{\pi^2}{4} \cdot \frac{K}{\log(L)}\right)}$$

where $c \leq 10^6$ is a universal constant and $\|B\|_{col}$, $\|C\|_{col}$ are the maximum column norm of the matrices B and C respectively.

In the following we prove the above theorem.

F.1. Proof of Theorem F.1

Without loss of generality we assume that A is a real-diagonal matrix. Before continuing with the proof, we will provide some requisite definitions and lemmas. Define the following vector for any α, $\mu(\alpha) \in \mathbb{R}^T$, with $\mu(\alpha)(i) = (\alpha^2 - 1)\alpha^{i-1}$. Further define the Hankel matrix H as

$$Z \triangleq \int_{-1}^{1} \mu(\alpha)\mu(\alpha)^\top d\alpha$$

As the following lemma shows the Hankel matrix Z above is the same Hankel matrix Z_L defined in the definition of STU (15).

Lemma F.2. *Z is a Hankel matrix with entries given as*

$$Z(i,j) = ((-1)^{i+j-2} + 1) \cdot \frac{8}{(i+j+3)(i+j-1)(i+j+1)}$$

Proof. Consider the following simple computations

$$\begin{aligned}
H(i,j) &= \int_{-1}^{1} (\alpha^2 - 1)^2 \alpha^{i+j-2} d\alpha \\
&= \int_{-1}^{0} (\alpha^2 - 1)^2 \alpha^{i+j-2} d\alpha + \int_{0}^{1} (\alpha^2 - 1)^2 \alpha^{i+j-2} d\alpha \\
&= \int_{-1}^{0} (|\alpha|^2 - 1)^2 (-1)^{i+j-2} |\alpha|^{i+j-2} d\alpha + \int_{0}^{1} (\alpha^2 - 1)^2 \alpha^{i+j-2} d\alpha \\
&= \int_{0}^{1} (\alpha^2 - 1)^2 (-1)^{i+j-2} \alpha^{i+j-2} d\alpha + \int_{0}^{1} (\alpha^2 - 1)^2 \alpha^{i+j-2} d\alpha \\
&= ((-1)^{i+j-2} + 1) \int_{0}^{1} (\alpha^2 - 1)^2 \alpha^{i+j-2} d\alpha \\
&= ((-1)^{i+j-2} + 1) \cdot \frac{8}{(i+j+3)(i+j-1)(i+j+1)}
\end{aligned}$$

□

Lemma F.3. *We have that the following statements hold regarding $\mu(\alpha)$ for any $\alpha \in [-1, 1]$,*

- $|\mu(\alpha)|^2 \leq 1$
- *For any $\alpha \in [-1, 1]$ and any unit vector v we have that*

$$(\mu(\alpha)^\top v)^2 \leq 6(v^\top Z v)$$

Proof. By definition $\mu(\alpha) = 0$ for $\alpha \in \{-1, 1\}$. Otherwise we have that for all $\alpha \in (-1, 1)$,

$$|\mu(\alpha)|^2 = \sum_{i=1}^{T} (\alpha^2 - 1)^2 \alpha^{2i-2} \leq \frac{(\alpha^2 - 1)^2}{(1 - \alpha^2)} = 1 - \alpha^2 \leq 1.$$

To prove the second part we consider drawing α from the uniform distribution between $[-1, 1]$. We get that

$$E[(\mu(\alpha)^\top v)^2] = \frac{v^\top Z v}{2}$$

We now show that the worst case value is not significantly larger than the expectation. To this end we consider the function $f(\alpha) = (\mu(\alpha)^\top v)^2$ and we show that this is a 6-Lipschitz function. To this end consider the following,

$$\begin{aligned}
\left\| \frac{\partial \mu(\alpha)}{\partial \alpha} \right\|_2^2 &= \sum_{i=0}^{T-1} \left\{ \left| \frac{\partial}{\partial \alpha} (1 - \alpha^2) \alpha^i \right|^2 \right\} \\
&= \sum_{i=0}^{T-1} \left((1 - \alpha^2) i \alpha^{i-1} - 2\alpha^{i+1} \right)^2 \\
&\leq 2(1 - \alpha^2)^2 \sum_{i=1}^{T-1} i^2 \alpha^{2(i-1)} + 4 \sum_{i=0}^{T-1} \alpha^{2i+2} && (a+b)^2 \leq 2(a^2 + b^2) \\
&\leq 2(1 - \alpha^2)^2 \left(\frac{1}{(1 - \alpha^2)^2} + \frac{2\alpha^2}{(1 - \alpha^2)^3} \right) + \frac{4\alpha^2}{1 - \alpha^2} && \sum_{i=1}^{\infty} i^2 \beta^{i-1} = \frac{1}{(1-\beta)^2} + \frac{2\beta}{(1-\beta)^3} \\
&= 2 + \frac{8\alpha^2}{(1 - \alpha^2)}.
\end{aligned}$$

Therefore we have that for all $\alpha \in [-1, 1]$,

$$\frac{\partial f(\alpha)}{\partial \alpha} = 2(\mu(\alpha)^\top v)\left(\frac{\partial \mu(\alpha)^\top}{\partial \alpha} v\right) \leq 2\|\mu(\alpha)\|\|v\|^2\|\frac{\partial \mu(\alpha)}{\partial \alpha}\|$$
$$\leq 2\sqrt{(1-\alpha^2) * \left(2 + \frac{8\alpha^2}{(1-\alpha^2)}\right)}$$
$$\leq 2\sqrt{2+6\alpha^2} \leq 6.$$

Now for the positive function $f(\alpha)$ which is 6-Lipschitz on $[-1, 1]$ let the maximum value be R. It can be seen the lowest expected value of $f(\alpha)$ over the uniform distribution over $[0, 1]$, one can achieve is $R^2/2 * 6$ and therefore we have that

$$R^2/12 \leq \frac{v^\top Z v}{2} \Rightarrow R \leq \sqrt{6 v^\top Z v},$$

which finishes the proof. □

A direct consequence of the above lemma is the following.

Lemma F.4. *For any $\alpha \in [0, 1]$, let $\tilde{\mu}(\alpha)$ be the projection of $\mu(\alpha)$ on the subspace spanned by top k eigenvectors of Z, then we have that*

$$\|\mu(\alpha) - \tilde{\mu}(\alpha)\|^2 \leq 6 \sum_{i=k+1}^{L} \sigma_i$$

Finally the following lemma with a proof similar to E.3 shows that the spectrum of the matrix Z decays exponentially.

Lemma F.5. *Let σ_j be the top j^{th} eigenvalue of Z. Then we have that*

$$\sigma_j \leq \Gamma c^{-j/\log(L)}$$

where $c = e^{\pi^2/4} \sim 11.79$ and $\Gamma = 235200$ is an absolute constant.

We now move towards proving Theorem F.1. Consider the following calculation for the LDS sequence y_t^{LDS}

$$y_t^{\text{LDS}} = \sum_{i=0}^{T} C A^i B u_{t-i} + D u_t,$$

and therefore we have that

$$y_t^{\text{LDS}} - y_{t-2}^{\text{LDS}} = (CB + D)u_t + CABu_{t-1} - Du_{t-2} + \underbrace{\sum_{i=0}^{T} C(A^{i+2} - A^i)Bu_{t-2-i}}_{\text{Term of Interest}}$$

For any $t_1 \geq t_2$ we define the matrix $\bar{U}_{t_1:t_2} \in \mathbb{R}^{d_{\text{out}} \times t_1 - t_2 + 1}$ whose i^{th} column is the input vector $u_{t_1 - i + 1}$. We allow t_2 to be negative and by convention assume $u_t = 0$ for any $t \leq 0$. Denote the diagonal entries of A by $\{\alpha_l\}_{l=1}^{d_h}$, i.e. $\alpha_l = A(l, l)$. The term of interest above can then be written as

$$\sum_{i=0}^{L} C(A^{i+2} - A^i)Bu_{t-2-i} = \sum_{l=1}^{d_h} (c_l \otimes b_l)\left(\sum_{i=0}^{L} (\alpha_l^{i+2} - \alpha_l^i) u_{t-2-i}\right)$$
$$= \sum_{l=1}^{d_h} (c_l \otimes b_l)\left(\sum_{i=0}^{L} (\alpha_l^2 - 1)\alpha_l^i u_{t-2-i}\right)$$
$$= \sum_{l=1}^{d_h} (c_l \otimes b_l)\left(\bar{U}_{\{t-2:t-1-L\}} \mu(\alpha)\right).$$

Therefore we get that

$$y_t^{\text{LDS}} - y_{t-2}^{\text{LDS}} = (CB + D)u_t + CABu_{t-1} - Du_{t-2} + \sum_{l=1}^{d_h} (c_l \otimes b_l) \left(\bar{U}_{\{t-2:t-1-L\}} \mu(\alpha) \right).$$

Recall that we defined the sequence $\{\sigma_k, \phi_k\}_{k=1}^{L}$ to be the eigenvalue and eigenvector pairs for the Hankel matrix Z. For any α we define the projection of $\mu(\alpha)$ on the top k eigenvectors as $\tilde{\mu}(\alpha)$, i.e. $\tilde{\mu}(\alpha) = \sum_{k=1}^{K} (\mu(\alpha_l)^\top \phi_k) \phi_k$. Further define STU parameters as follows

$$M_1^u = CB + D, M_2^u = CAB, M_3^u = -D$$

$$M_k^\phi = \sum_l (\mu(\alpha_l)^\top \phi_k) \sigma_k^{-1/4} (c_l \otimes b_l)$$

The definition of STU prediction (using the above parameters) implies that the predicted sequence satisfies

$$y_t^{\text{STU}} - y_{t-2}^{\text{STU}} = (CB + D)u_t + CABu_{t-1} - Du_{t-2} + \sum_l (c_l \otimes b_l) \left(\bar{U}_{\{t-2:t-1-L\}} \right) \left(\underbrace{\sum_{k=1}^{K} (\mu(\alpha_l)^\top \phi_k) \phi_k}_{=\tilde{\mu}(\alpha)} \right).$$

Combining the above displays we get that

$$y_t^{\text{LDS}} - y_t^{\text{STU}} = y_{t-2}^{\text{LDS}} - y_{t-2}^{\text{STU}} + \sum_l (c_l \otimes b_l) \left(\bar{U}_{\{t-2:t-1-L\}} \right) \left(\mu(\alpha) - \tilde{\mu}(\alpha) \right).$$

Using a similar derivation as in the proof of Theorem 2.1 we get that

$$\|y_t^{\text{LDS}} - y_t^{\text{STU}}\| \leq \|y_{t-2}^{\text{LDS}} - y_{t-2}^{\text{STU}}\| + 10 \cdot \|B\|_{\text{col}} \cdot \|C\|_{\text{col}} \cdot L^{1.5} \cdot a \cdot \sqrt{\sum_{i=K+1}^{L} \sigma_i}$$

Applying the above equation recursively and Lemma F.5 we get that for any $K \geq \log(L)$

$$\|y_t^{\text{LDS}} - y_t^{\text{STU}}\| \leq 5 \cdot \|B\|_{\text{col}} \cdot \|C\|_{\text{col}} \cdot L^{2.5} \cdot a \cdot \sqrt{\sum_{i=K+1}^{L} \sigma_i} \leq c \cdot \|B\|_{\text{col}} \cdot \|C\|_{\text{col}} \cdot L^{3} \cdot a \cdot e^{\left(-\frac{\pi^2}{4} \cdot \frac{K}{\log(L)} \right)}.$$

where $c = 2.5 \times \Gamma \leq 10^6$ is an absolute constant. This finishes the proof of the theorem.

G. Experiment Details

G.1. Synthetic Experiments with a marginally-stable LDS

The random system we generated for the experiments displayed in Figure 3a is as follows -

$$A = \begin{bmatrix} -0.9999 & 0. & 0. & 0. \\ 0. & 0.9999 & 0. & 0. \\ 0. & 0. & -0.9999 & 0. \\ 0. & 0. & 0. & 0.9999 \end{bmatrix}, \quad B = \begin{bmatrix} 0.36858183 & -0.34219486 & 0.1407376 \\ 0.18933886 & -0.1243964 & 0.21866894 \\ 0.14593862 & -0.5791096 & -0.06816235 \\ -0.3095346 & -0.21441863 & 0.08696061 \end{bmatrix}$$

$$C = \begin{bmatrix} 0.5528727 & -0.51329225 & 0.21110639 & 0.2840083 \\ -0.18659459 & 0.3280034 & 0.21890792 & -0.8686644 \\ -0.10224352 & -0.46430188 & -0.32162794 & 0.1304409 \end{bmatrix}, \quad D = \begin{bmatrix} 1.5905786 & 0. & 0. \\ 0. & -0.45901108 & 0. \\ 0. & 0. & 0.3238576 \end{bmatrix}$$

Hyperparameters for STU: We only tuned the learning rate in the set ($[5e-2, 1e-1, 5e-1, 1, 5, 10]$) for vanilla STU and used $K = 25$.

Hyperparameters for LRU:

- **Model Hyperparameters** (Orvieto et al., 2023) provide a few recommendations for the LRU model. We tested exhaustively over the following hyperparameter choices:
  - Stable Exp-parameterization: We searched over [True, False]
  - Logarithmic Representation of Recurrent Parameters: We searched over [True, False]
  - γ-Normalization: We searched over [True, False]
  - Ring Initialization: We searched over `min_rad`$\in \{0.0, 0.9, 0.99, 0.999\}$ and `max_rad`$\in \{0.9, 0.99, 0.999, 1.0\}$.
  - Setting the `max_init_phase`$\in \{1.57, 3.14, 6.28\}$

  We found the Stable Exp-parameterization, Logarithmic Representation of Recurrent Parameters and γ-normalization to be essential for training in this problem. We did not observe any particular benefit of Ring Initialization or reducing the phase at initialization and we set them to defaults eventually. We provide the learning curves over our search space in Figure 5.

- **Optimization Hyperparameters** Given the comparatively higher sample complexity of the LRU model we employed standard deep-learning optimization tricks like tuning weight-decay as well as applying a cosine learning rate schedule with warmup. These optimization tricks did not lead to gains over standard training with Adam and a fixed learning rate in this problem. We tuned the learning rate in the set ($[5e-2, 1e-1, 5e-1, 1, 5, 10]$).

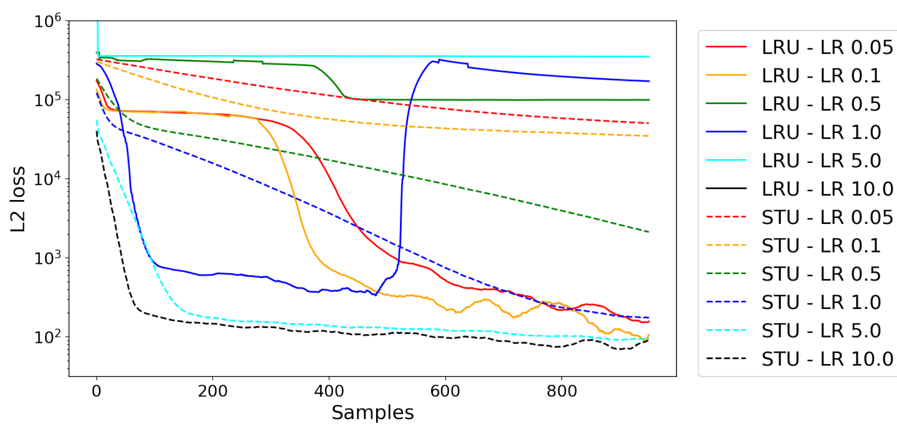

Figure 4: (Smoothed) Learning curves for learning a marginally stable LDS for a single STU layer (dashed) vs a single LRU layer (solid). Different colors represent different learning rates highlighting that the training becomes unstable for LRUs quickly as LR increases while the STU trains at much higher learning rates. Curiously at stable LRs we observe that LRUs show a platea-ing of learning for a large fraction of the training time.

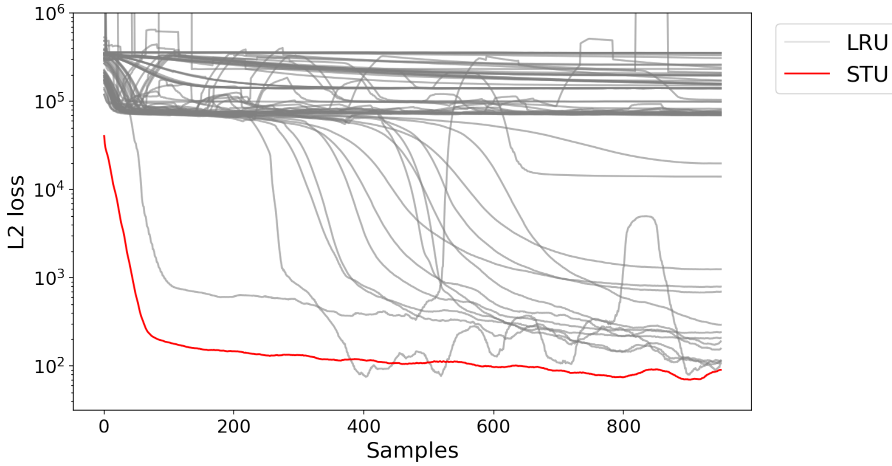

Figure 5: LRU Hparam search vs STU. All the gray curves represent the hyperparameters for LRU we tried. The STU curve is the best taken from Figure 4. For LRU we searched over choices of enabling stable exp-parameterization, gamma-normalization, ring-initialization, phase-initialization, learning rate, weight decay and constant vs warmup+cosine decay lr schedule.

G.2. Experimental setup for LRA experiments

Our training setup closely follows the experimental setup used by (Orvieto et al., 2023). We use the same batch sizes and training horizons for all the tasks as employed by (Orvieto et al., 2023).

Hyperparameter tuning For all of our experiments on the LRA benchmark for both the vanilla STU model and the auto-regressive AR-STU model we searched the learning rate in the set $\{1e-4, 3e-4, 5e-4, 1e-3, 2.5e-3, 5e-3\}$ and tune the weight decay in the set $\{1e-3, 1e-2, 1e-1, 5e-1, 1.0\}$. We fix the number of filters K to be 24. We use Adam as the training algorithm with other optimization hyperparameters set to their default values. We use the same learning rate schedule as (Orvieto et al., 2023), i.e. 10% warmup followed by cosine decay to 0. For the AR-STU model we searched over two values of $k_y \in \{2, 32\}$. In Table 2 we present a comparison of vanilla STU with AR-STU with $k_y = 2$ and AR-STU with $k_y = 32$. We find that both vanilla STU and AR-STU $k_y = 2$ reach comparable accuracy which is better than the baselines S4 and LRU on non-image datasets. On image datasets we found $k_y = 32$ to be helpful in getting better test accuracies.

Initialization For the STU model we initialized **all** the M matrices at 0.

Finally while training the AR-STU model as employed by the training setup of (Orvieto et al., 2023) and previous SSM implementations, we found that using a smaller value of LR specifically for M^y matrices to be useful. We decreased the value of LR by a factor 0.1 or 0.05 and searched over this parameter.

H. Power of Auto-regression: Dimension-dependent representation for LDS

In this section we give a short proof that any partially-observed LDS can be perfectly predicted via a linear predictor acting over at most d of its past inputs and outputs where d is the hidden-state dimensionality (i.e. $A \in \mathbb{R}^{d\times d}$). In particular

Theorem H.1. *Given an LDS parameterized by $A \in \mathbb{R}^{d\times d}, B, C, D$, there exist coefficients $\alpha_{1:d}$ and matrices $\Gamma_{0:d}$ such that given any input sequence $u_{1:L}$, the output sequence $y_{1:L}$ generated by the action of the LDS on the input satisfies for all t*

$$y_t = \sum_{i=1}^{d} \alpha_i y_{t-i} + \sum_{i=0}^{d} \Gamma_i u_{t-i}$$

Proof. By unrolling the LDS we have that $y_t = \sum_{i=0}^{t} CA^i B u_{t-i} + D u_t$.. By the Cayley Hamilton theorem, the matrix A

	CIFAR	ListOps	Text	Retrieval	Pathfinder	PathX
S4 (Gu et al., 2021a)	88.65	59.60	86.82	90.90	94.20	96.35
LRU (Orvieto et al., 2023)	89	60.2	89.4	89.9	95.1	94.2
STU	83.73	61.04	**90.48**	90.40	91.70	89.71
AR-STU ($k_y = 2$)	86.56	**61.14**	**90.47**	90.52	93.85	90.49
AR-STU ($k_y = 32$)	**91.34**	57.66	88.51	87.39	**95.45**	93.24

Table 2: Comparison of the STU model against various proposed SSM models on the LRA benchmark: Bold values indicate the best for that task. We find that STU is competitive across all the workloads without the need for carefully designed initializations, discretizations or normalizations. We report the median over 5 trials for our experiments.

has a characteristic polynomial p of degree d, namely there exists d numbers $c_{1:d}$ such that

$$p(z) = \sum_{i=0}^{d} c_i z^i$$

satisfies $p(A) = 0$. Without loss of generality we can assume the constant term in the polynomial is 1. We can now consider the series for $y_t, y_{t-1}, \ldots$ as

$$\begin{array}{lcllll} y_t - Du_t & = & CBu_t & CABu_{t-1} & \ldots & CA^t Bu_1 \\ y_{t-1} - Du_{t-1} & = & 0 & CBu_{t-1} & \ldots & CA^{t-1}Bu_1 \\ \vdots & & & & & \\ y_{t-d} - Du_{t-d} & = & 0 & 0 & \ldots & CA^{t-d}Bu_1 \end{array}$$

Now, if we take the combination of the above rows according to the coefficients of the characteristic polynomial, we get that

$$\sum_{i=0}^{d} c_i y_{t-i} = \sum_{j=0}^{t} R_j + \sum_{i=0}^{d} Du_{t-i} \tag{17}$$

where R_j is the appropriate sum along the $j'th$ column of the matrix above. For all $j > d$, this amounts to an expression of the form:

$$j > d \ \Rightarrow \ R_j = \sum_{i=0}^{d} c_i CA^i \cdot A^{t-j}Bu_{t-j} = C(\sum_{i=0}^{d} c_i A^i) \cdot A^{t-j}Bu_{t-j} = C \cdot p(A) \cdot A^{t-j}Bu_{t-j} = 0.$$

Since all but the first d columns are zero, rearranging (17) and collecting terms, we get that there exists coefficients $\alpha_{1:d}$ and matrices $\Gamma_{0:d}$ such that

$$y_t = \sum_{i=1}^{d} \alpha_i y_{t-i} + \sum_{j=0}^{d} \Gamma_j u_{t-j}.$$

□